Prospects of searching for excited leptons during run II of the Fermilab Tevatron

E. Boos,[1] A. Vologdin,[1] D. Toback,[2] and J. Gaspard[2]
[1]*Institute of Nuclear Physics, Moscow State University, 119899, Moscow, Russia*
[2]*Texas A & M University, College Station, Texas 77843*
(Received 9 April 2002; published 30 July 2002)

We present the prospects of searching for excited leptons during run II of the Fermilab Tevatron. We concentrate on single and pair production of excited electrons in the photonic decay channel for both 2 fb^{-1} (run IIa) and 15 fb^{-1} (run IIb) using one CDF or DØ detector equivalent. We expect the Tevatron to improve upon the limits set by CERN LEP and DESY HERA for excited lepton masses above 190 GeV by the end of run IIa.

DOI: 10.1103/PhysRevD.66.013011 PACS number(s): 13.10.+q, 12.60.Rc, 13.85.Rm, 14.60.Hi

The standard model (SM) of particle physics is known to give results that match the current experimental data with high precision. However, because of well known theoretical problems and disadvantages, it is widely believed that it cannot be a complete theory of elementary particles, but rather an effective theory at energies below some scale on the order of a TeV. While many models of ''new physics'' beyond the SM have been suggested over the years, one of the most straightforward ideas proposes that quarks and leptons are composite particles. Such models can explain, in principle, family replication, mixing in the quark and lepton sectors, and make the fermion masses and weak mixing angles calculable.

In most composite models fermions possess an underlying substructure which is characterized by a scale Λ, with Λ about 1 TeV or higher [1]. While there is no unified model of compositeness [2], a model-independent effective Lagrangian for excited leptons l^*, originally proposed in Ref. [3], can be used to model single and pair production in experiments. The Lagrangian terms

$$L_{l^*l^*}=\bar{l}^*\gamma^\mu\left(\frac{\tau}{2}W_\mu+g'\frac{Y}{2}B_\mu\right)l^* \tag{1}$$

$$L_{l^*l}=\frac{1}{2\Lambda}\bar{l}_R^*\sigma^{\mu\nu}\left(fg\frac{\tau}{2}W_{\mu\nu}+f'g'\frac{Y}{2}B_{\mu\nu}\right)l_L + \mathrm{H.c.}, \tag{2}$$

where f and f' are coupling constants, have been used extensively in a number of phenomenological papers which present ideas on searching for excited fermion production and decay to final state gauge bosons in e^+e^-, $p\bar{p}$, ep, and $e\gamma$ collisions [4–6]. Direct searches for lepton compositeness have been done extensively at the CERN e^+e^- collider LEP [7] and the DESY ep collider HERA [8], each with no discovery, but with ever more sensitive limits. Unfortunately, only direct searches for quark compositeness have been done at the Fermilab Tevatron [9].

In this paper we present a study of the discovery potential for compositeness by searching for excited lepton production and decay in run II of the Tevatron using the Collider Detector at Fermilab (CDF) and DØ detectors [10]. We begin with an updated simulation of excited lepton production, and optimize the sensitivity by studying the kinematics of excited lepton production and decay relative to SM backgrounds. With these results we estimate the mass reach and compare it to the recent results from LEP and HERA.

To study the mass reach of the Tevatron, we simulated single and pair production and the decay of excited leptons using the upgraded Fermilab accelerator (1.8→2.0 TeV), and the CDF and DØ detectors [10] for run II. The Feynman rules from the effective Lagrangians [Eqs. (1) and (2)] are implemented in COMPHEP [11] using the LANHEP [12] software package. We have included into this simulation a complete tree-level calculation which takes into account all the spin correlations between excited state production and subsequent decays, with the known next-to-leading-order corrections incorporated. All the partial widths and known $2\rightarrow2$ cross sections have been cross-checked at the symbolic level. Events at parton level are generated by means of COMPHEP as an external process for PYTHIA [13] with the help of the COMPHEP-PYTHIA interface [14]. The underlying event, jet fragmentation, initial state radiation and final state radiation are modeled using the PYTHIA Monte Carlo program with the CTEQ4L [15] structure functions. Since Drell-Yan production of excited leptons is similar to that of supersymmetric leptons, we take the K factors given in Ref. [16], which only depend on the masses of final particles, and vary between 1.23 and 1.24 in the mass range between 150 and 300 GeV.

While excited leptons can come in three flavors, e^*, μ^* and τ^*, we chose to concentrate on the electron channel since the results for μ^*'s are expected to be similar to those for e^*'s, and τ's at the Tevatron are still difficult to trigger on and identify. Excited electrons can decay via $e^*\rightarrow e\gamma$, $e^*\rightarrow eZ$ and $e^*\rightarrow W\nu$ with branching ratios $\mathcal{B}(e^*\rightarrow e\gamma)$, $\mathcal{B}(e^*\rightarrow \nu W)$ and $\mathcal{B}(e^*\rightarrow eZ)$ as shown in Fig. 1. Searching for the W and Z decays at the Tevatron is problematic; the backgrounds to these channels are large, and the leptonic branching fractions are small. However, photons are directly identified and the backgrounds to the photonic final states are relatively small, especially in our mass range of interest. This makes them a gold-plated signature.

In the case of single $e^*\rightarrow e\gamma$ production there are two possible signals, $p\bar{p}\rightarrow e^*e\rightarrow ee\gamma$ and $p\bar{p}\rightarrow e^*\nu\rightarrow e\nu\gamma$.

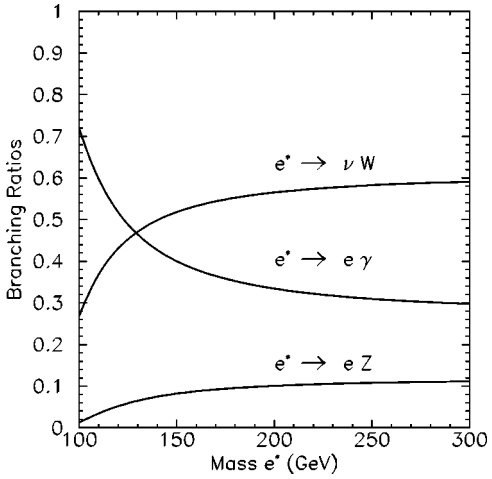

FIG. 1. The branching ratios for excited electrons as a function of the mass of the excited electron.

Similarly, pair production gives $p\bar{p}\rightarrow e^*e^*\rightarrow ee\gamma\gamma$ and $p\bar{p}\rightarrow e^*\nu^*\rightarrow e\nu\gamma\gamma$. We concentrate on the inclusive $ee\gamma$ final state as single production dominates over pair production by about a factor of 10^3, and backgrounds to $ee\gamma$ are smaller than for $e\nu\gamma$. We simulate both single and pair production mechanisms for our estimates. Since only the production cross section and not the kinematics of the system are dependent on f/Λ and f' we choose, for simplicity, $f/\Lambda = 10^{-2}$ GeV^{-1} and $f=f'$. Figure 2 shows the total and visible $ee\gamma$ production cross sections for this case.

There are a number of backgrounds to the $ee\gamma$ channel. The dominant backgrounds are $W\gamma+$jets and $Z\gamma+$jets production. Others include $W+$jets, $Z+$jets, and multijets, where jets can fake leptons and/or photons. Studies have shown [17] that the fake backgrounds can be modeled using the kinematics of the diboson irreducible backgrounds. We

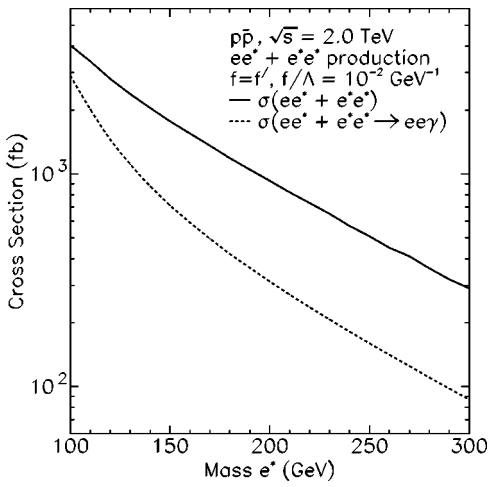

FIG. 2. The excited lepton production cross section at the Fermilab Tevatron. The solid line shows the total cross sections for the sum of both single and pair production and decay of excited electrons. The dashed line shows the visible cross section in the $ee\gamma$ final state.

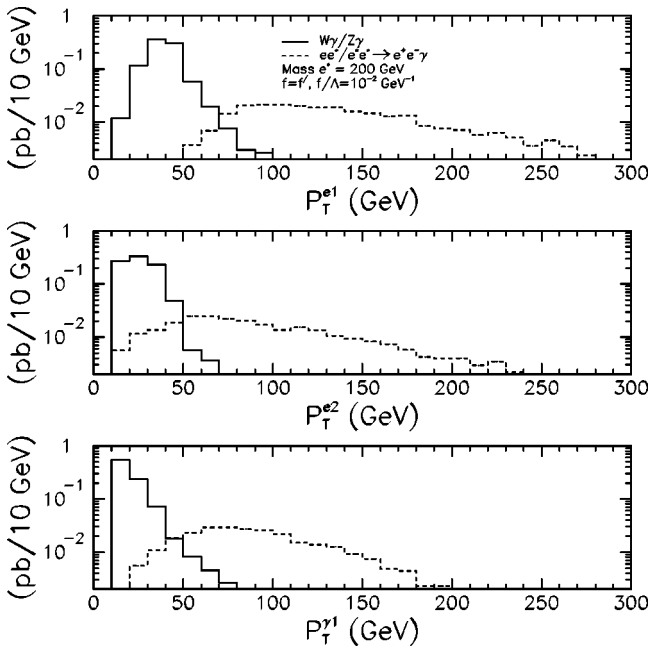

FIG. 3. A comparison of the p_T distributions of the final state electrons (e_1 and e_2) and the photon (γ_1) for $e^*e\rightarrow ee\gamma$ and $e^*e^*\rightarrow ee\gamma$ production, and for standard model background processes. One can see that kinematics are well separated for large values of p_T.

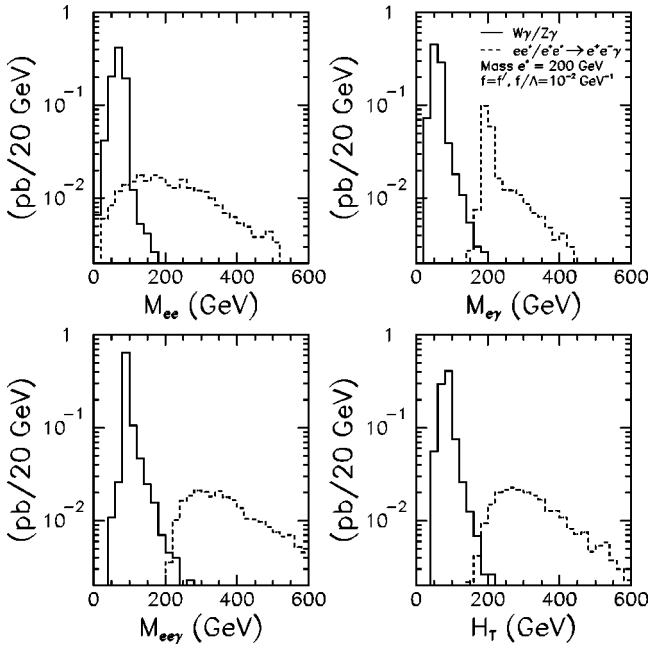

FIG. 4. A comparison of some of the variables studied which give good separation between excited leptons ($M_{e*}=200$ GeV) and the standard model background processes ($W\gamma$ and $Z\gamma$) in the $ee\gamma$ final state. H_T is the scalar sum of the p_T's of all the electrons and photons in the event. Note that the $M_{e\gamma}$ variable gives the best separation between signal and background and the optimal cut, as described in Table I, is $M_{e\gamma}>185$ GeV.

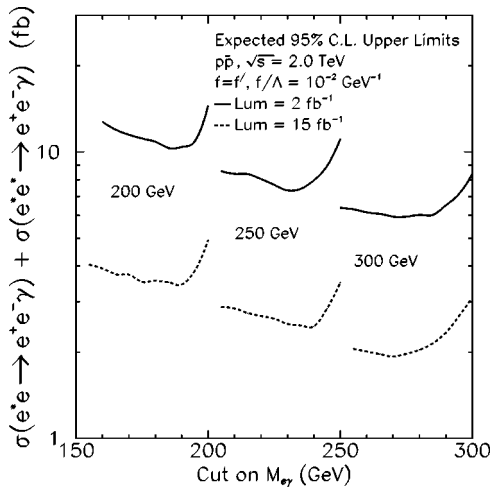

FIG. 5. The average expected 95% C.L. cross-section upper limit $\sigma_{95}^{\mathrm{avg}}(cut)$, as a function of the $M_{e\gamma}$ cut for different masses of e^*. The minimum value for each M_{e*} is the optimal limit $\sigma_{95}^{\mathrm{exp}}$. The solid line and dashed line show the results for 2 fb^{-1} and 15 fb^{-1} of data respectively.

use the same COMPHEP simulation structure described above. Since there is an infrared singularity at $p_T^{\gamma}=0$, at the generator level we require $p_T^{\gamma}>10$ GeV and $\Delta R_{ij}>0.1$, where $\Delta R_{ij}\equiv\sqrt{(\Delta\eta)^2+(\Delta\varphi)^2}$, and i and j are any lepton-photon combination. We take the K factor, which has a value of about 1.36 depending on p_T^{γ}, for the background processes from the literature [18].

For both signal and backgrounds we use a parametric simulation to model the detector response. The SHW detector simulation [19] has been shown to be an effective averaging between the CDF and DØ detectors [10] for run II. After detector simulation the kinematic distributions for both the signal and estimated backgrounds are shown in Figs. 3 and 4. We require each e and γ to have $p_T>10$ and $|\eta|<1.5$ for

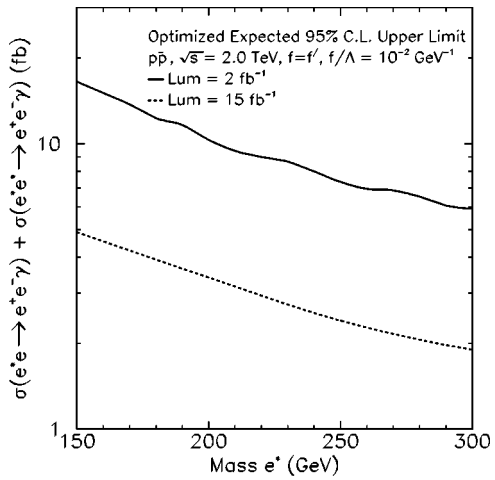

FIG. 6. The optimized expected 95% C.L. for cross-section upper limits $\sigma_{95}^{\mathrm{exp}}$, for $e^*\to e\gamma$ production using the $ee\gamma$ final state. The solid and dashed lines show the results for 2 fb^{-1} and 15 fb^{-1} of data respectively.

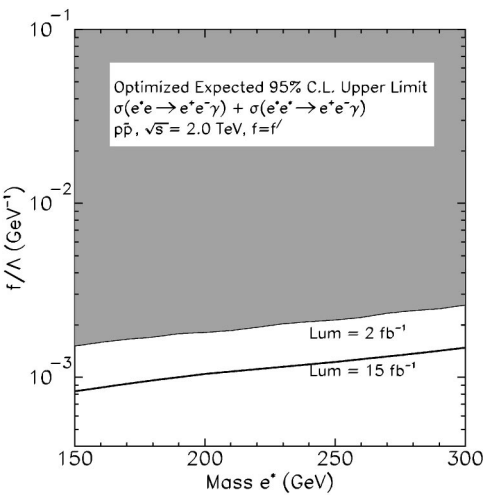

FIG. 7. Exclusion plot for f/Λ as a function of e^* mass. The solid shaded region and the solid line show the exclusions for 2 fb^{-1} and 15 fb^{-1} worth of data respectively.

electrons and $|\eta|<2$ for photons. For e^* masses above 150 GeV we find acceptances at about the 0.5 level, and that the signal is easily separated from the background in many kinematic distributions.

To maximize our sensitivity we assume, for simplicity, that taking a set of data selection requirements (cuts) which minimizes the expected cross section limit at 95% confidence level (C.L.), $\sigma_{95}^{\mathrm{exp}}$, also maximizes our sensitivity for discovery. To calculate the expected limits we use the signal acceptance and background estimates from the simulations above, each taken with 10% systematic error, and assume a single detector for two scenarios: 2 fb^{-1} and 15 fb^{-1} of luminosity, taken with 5% sytematic uncertainty. If there is no signal in the data the limit is uniquely determined by the number of events observed in the data, the acceptance, the expected background rate and the sample luminosity. We use

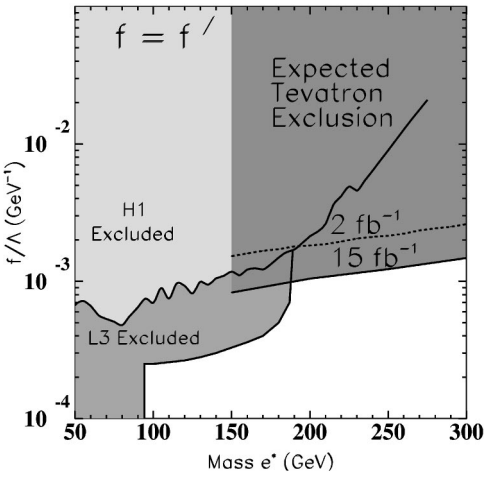

FIG. 8. Exclusion plot for f/Λ as a function of e^* mass. For masses above about 190 GeV, we expect that the Tevatron should, with 2 fb^{-1} of data and one detector, produce the most stringent limits. With 15 fb^{-1} these limits would be extended to significantly lower values of f/Λ.

TABLE I. Optimized expected 95% C.L. cross-section upper limits on the production and decay of $e^* \to e\gamma$. Note that all results are for 2 fb^{-1}, $f/\Lambda = 10^{-2}$ GeV^{-1} and $f = f'$. Here σ^{Total} is the total e^*e and e^*e^* production and $\sigma^{ee\gamma}$ is the visible $ee\gamma$ cross section as shown in Fig. 2. $M_{e\gamma}^{\text{cut}}$ is the optimized selection requirement on the $e\gamma$ mass. For the cut listed, N_{back} is the number of background events from $W\gamma$ and $Z\gamma$ sources for this cut, and Accept is the acceptance.

M_{e^*} (GeV)	σ^{Total} (fb)	$\mathcal{B}(e^* \to e\gamma)$	$\sigma^{ee\gamma}$ (fb)	$M_{e\gamma}^{\text{cut}}$ (GeV)	N_{back}	Accept	σ_{95}^{exp} (fb)	$\sigma_{95}^{\text{exp}} \cdot \mathcal{B}$ (fb)
150	1,770	0.400	712	140	42.0	0.54	41.3	16.5
200	930	0.334	312	185	18.0	0.56	30.9	10.3
250	510	0.309	160	230	7.64	0.57	23.7	7.3
300	290	0.297	87	275	4.36	0.56	20.0	5.9

a frequentist method [20] to incorporate the errors and assume that all errors on acceptance, background and luminosity are uncorrelated. Explicitly, the limit is a function of the cuts and the number of events observed in the data N, and can be written as $\sigma_{95}(N,cut)$. With the assumption of no observed signal, N fluctuates around the mean number of expected background events M, according to Poisson statistics. In this way we estimate an average expected cross-section limit as a function of each cut, $\sigma_{95}^{\text{avg}}(cut)$. Specifically,

$$\sigma_{95}^{\text{avg}}(cut) = \sum_{N=0}^{\infty} \sigma_{95}(N,cut) \frac{e^{-M} M^N}{N!}. \tag{3}$$

We find the expected optimal limit, σ_{95}^{exp}, for each mass point by finding the minimum of the distribution as a function of the cut,

$$\sigma_{95}^{\text{exp}} = [\sigma_{95}^{\text{avg}}(cut)]_{\text{min}}. \tag{4}$$

We have studied $\sigma_{95}^{\text{avg}}(cut)$ as a multi-variable function of the kinematical distributions in Figs. 3 and 4. We find that applying a cut on the single kinematical variable $M_{e\gamma}$ (where e is the electron with highest p_T) gives the minimal value of σ_{95}^{exp} for a given mass of the excited electron. This is prominent in Figs. 3 and 4, showing that the best separation between signal and background is the $M_{e\gamma}$ variable. Figure 5 shows the expected 95% C.L. cross section upper limit $\sigma_{95}^{\text{avg}}(cut)$ as a function of the $M_{e\gamma}$ cut for different masses of e^* for $f/\Lambda = 10^{-2}$ GeV^{-1} and $f = f'$. Placing our cut at the minimum of each curve gives the final expected cross section limit, σ_{95}^{exp}. Since the minimum cut value is virtually identical for both 2 fb^{-1} and 15 fb^{-1}, we quote the results using the cuts for 2 fb^{-1}. Both results are shown in Fig. 6 and the 2 fb^{-1} results are tabulated in Table I, along with more detail about the optimal cut values, final acceptances and expected backgrounds for each.

In order to set more general limits on the excited lepton production, we use the Feynman rules for the Lagrangian in Eq. (2) (since single production dominates for all values of f/Λ of interest) which give a simple relation between cross-section limits and f/Λ for signal. Specifically, we find,

$$(\Lambda_1)^2 \sigma\left(\frac{f}{\Lambda_1}, M_{e^*}\right) = (\Lambda_2)^2 \sigma\left(\frac{f}{\Lambda_2}, M_{e^*}\right). \tag{5}$$

Using this equation, numerical values of the cross-section limits σ_{95}^{exp}, and $f/\Lambda = 10^{-2}$ GeV^{-1} (for which σ_{95}^{exp} was calculated), we find

$$\left(\frac{f}{\Lambda}\right)^2 = \frac{\sigma_{95}^{\text{exp}}}{10^4 \sigma(10^{-2}, M_{e^*})}. \tag{6}$$

This allows us to convert the limits in Fig. 6 into the exclusion plot in the f/Λ vs M_{e^*} plane as shown in Fig. 7. We compare our results for both 2 fb^{-1} and 15 fb^{-1} to those of LEP and HERA in Fig. 8. With just 2 fb^{-1} of data a single detector would give the most stringent limits, to date, for masses above about 190 GeV. A luminosity of 15 fb^{-1} would significantly extend the exclusion for the same mass region into smaller values of f/Λ.

The prospects for searching for excited electrons in the $e\gamma$ final state at the upgraded Fermilab Tevatron are excellent. We expect that with a single detector and 2 fb^{-1} of data we should be able to significantly extend the mass reach, especially in the low f/Λ region for masses above 190 GeV, and further extend them for 15 fb^{-1}. We also expect similar results for excited muons because the CDF and DØ detectors have similar leptonic coverage. This would significantly improve on the current μ^* limits, which are not producible at HERA.

The authors would like to thank John Hobbs for the use of his limit calculator, Bruce Knuteson for his relation in Eq. (3), and Bhaskar Dutta for helpful discussions. We would also like to thank the DØ Collaboration for the use of their computers to do the simulation work. We also would like to thank the Institute of Nuclear Physics of Moscow State University, the University of Maryland, and Texas A&M University for their support. We would like to thank the U.S. DOE and Russian Ministry of Industry, Science and Technology for their support during this project. The work of E.B. and A.V. was partly supported by the RFBR 01-02-16710, CERN-INTAS 99-377, and INTAS 00-0679 grants. E.B. thanks the Humboldt Foundation for financial support.

[1] Current experimental constraints come from the analysis of the g-2 properties of muon and electron, and from the estimate of quark and lepton radii. See A. Czarnecki and W.J. Marciano, talk given at the Fifth International Symposium on Radiative Corrections, RADCOR 2000, Carmel, California, 2000, hep-ph/0010194; K. Lane, hep-ph/0102131.

[2] For example the existence of excited states may be the result of the quark, lepton and boson fields propagating in extra dimensions. In that case one would expect the appearance of excited states in pairs as discussed in T. Appelquist, H. Cheng, and B.A. Dobrescu, Phys. Rev. D **64**, 035002 (2001).

[3] K. Hagiwara *et al.*, Z. Phys. C **29**, 115 (1985).

[4] F. Boudjema *et al.*, Z. Phys. C **57**, 425 (1993).

[5] U. Baur *et al.*, Phys. Rev. D **42**, 815 (1990).

[6] S. Belyaev and E. Boos, Yad. Fiz. **56N11**, 5 (1993) [Phys. At. Nucl. **56**, 1447 (1993)].

[7] ALEPH Collaboration, R. Barate *et al.*, Eur. Phys. J. C **4**, 571 (1998); DELPHI Collaboration, P. Abreu *et al.*, *ibid.* **8**, 41 (1999); OPAL Collaboration, G. Abbiendi *et al.*, *ibid.* **14**, 73 (2000); L3 Collaboration, M. Acciarri *et al.*, Phys. Lett. B **502**, 37 (2001).

[8] ZEUS Collaboration, J. Breitweg *et al.*, Z. Phys. C **76**, 631 (1997); H1 Collaboration, C. Adloff *et al.*, Eur. Phys. J. C **17**, 567 (2000).

[9] DØ Collaboration, B. Abbott *et al.*, Phys. Rev. Lett. **82**, 2457 (1999); DØ Collaboration, B. Abbott *et al.*, *ibid.* **80**, 666 (1998); DØ Collaboration, B. Abbott *et al.*, Phys. Rev. D **62**, 031101(R) (2000); CDF Collaboration, F. Abe *et al.*, Phys. Rev. Lett. **71**, 2542 (1993).

[10] T. LeCompte and H. Diehl, Annu. Rev. Nucl. Part. Sci. **50**, 71 (2000).

[11] E.E. Boos *et al.*, hep-ph/9503280; P. Baikov *et al.*, in *Workshop on High Energy Physics and Quantum Field Theory*, edited by B. Levtchenko and V. Savrin (Moscow University Press, Moscow, 1996), p. 101; A. Pukhov *et al.*, hep-ph/9908288.

[12] A. Semenov, Nucl. Instrum. Methods Phys. Res. A **393**, 293 (1997); A. Semenov, hep-ph/9608488.

[13] T. Sjöstrand, Comput. Phys. Commun. **82**, 74 (1994); S. Mrenna, *ibid.* **101**, 232 (1997); T. Sjöstrand, P. Eden, C. Friberg, L. Lonnblad, G. Miu, S. Mrenna, and E. Norrbin, *ibid.* **135**, 238 (2001).

[14] A.S. Belyaev *et al.*, in the Proceedings of the Seventh International Workshop on Advanced Computing and Analysis Techniques in Physics Research, ACAT2000, Fermilab, 2000, hep-ph/0101232.

[15] H.L. Lai *et al.*, Phys. Rev. D **55**, 1280 (1997).

[16] H. Baer *et al.*, Phys. Rev. D **57**, 5871 (1998).

[17] DØ Collaboration, F. Abachi *et al.*, Phys. Rev. Lett. **75**, 1023 (1995).

[18] J. Smith *et al.*, Z. Phys. C **44**, 267 (1989).

[19] The Supersymmetry/Higgs Workshop, Version 2.3, Fermilab, Batavia, Illinois, http://fnth37.fnal.gov/susy.html

[20] G. Zech, Nucl. Instrum. Methods Phys. Res. A **227**, 608 (1989); T. Huber *et al.*, Phys. Rev. D **41**, 2709 (1990).